Relation of Neural Response to Palatable Food Tastes and Images to Future Weight Gain: Using Bootstrap Sampling to Examine Replicability of Neuroimaging Findings

E Stice[1,*] and **S Yokum**[1]

[1]Oregon Research Institute, 1776 Millrace Drive, Eugene, Oregon, 97403

Abstract

Because understanding neural vulnerability factors that predict future weight gain may guide the design of more effective obesity prevention programs and treatments, we tested whether neural response to palatable food tastes and images predicted future weight gain. We recruited 135 initially healthy weight adolescents, to reduce the possibility that a history of overeating affected neural responsivity, had them complete fMRI paradigms examining neural response to tastes of milkshakes that varied in fat and sugar content and images of palatable foods, and assessed BMI annually over a 3-year follow-up. We used a novel bootstrapping analytic approach to investigate the replicability of the fMRI findings. Whole-brain analyses indicated that lower response in the pre-supplemental motor area to high-fat/low-sugar milkshake taste predicted future BMI gain in the full sample and in 5 out of the 10 bootstrap samples. Elevated response in the precentral gyrus/ Rolandic operculum to images of appetizing foods predicted future BMI gain in the full sample and in 4 out of the 10 bootstrap samples. Other peaks that emerged in the full sample did not replicate in most of the bootstrap samples, suggesting they were not reliable. Region of interest analyses did not replicate the predictive effects of peaks reported in past papers that used similar paradigms, including the evidence that *TaqIA* polymorphism moderated the relation of striatal response to palatable food tastes to future weight gain. Results suggest that lower responsivity of a region implicated in motor processing in response to palatable taste was associated with greater BMI gain over time, and further that bootstrap sampling may be useful for estimating the replicability of findings that emerge from whole brain analyses or regions of interest analyses with the full sample.

1. Introduction

Obesity results in 2.8 million deaths annually (World Health Organization, 2013), but treatments rarely produce lasting weight loss (Turk et al., 2009). An understanding of neural vulnerability factors that predict future weight gain may inform the design of more effective

*Correspondence: Eric Stice, Oregon Research Institute, 1776 Millrace Drive, Eugene, OR 97403, Phone: (541) 484-2123, Fax: (541) 484-1108, estice@ori.org.

obesity prevention programs and treatments. Palatable food intake and images activate brain regions implicated in reward (e.g., striatum, midbrain, amygdala, orbitofrontal cortex [OFC]) and cause striatal dopamine (DA) release that correlates with meal pleasantness and the caloric density of the food (Ferreira et al., 2012; Small et al., 2003), prompting a focus on individual differences in reward region responsivity.

Few studies have examined neural vulnerability factors that predict future weight gain, which ensures that they are precursors of overeating. Elevated OFC response to cues that predict palatable food image presentation (Yokum et al., 2011), elevated nucleus accumbens response to palatable food images (Demos et al., 2012), and elevated caudate response to palatable food commercials (Yokum et al., 2014), predicted future weight gain, though another study did not replicate these main effects (Stice et al., 2010). Geha and associates (2013) found that elevated amygdala, midbrain, hypothalamus, thalamus, ventral pallidum, and nucleus accumbens response to high-calorie beverage tastes predicted future weight gain, but another study did not find a main effect between greater reward region response to high-calorie beverage taste and future weight gain (Stice et al., 2008a). The mixed findings may have emerged because these studies used small samples sizes, which increases risk for chance findings that do not replicate. The fact that many of these studies predicted weight gain over short follow-ups may also have contributed to the unreliability of findings. Accordingly, we conducted a larger study with 162 healthy weight adolescents, which allowed us to conduct split-half analyses, in which we tested whether similar effects emerged in two randomly selected halves of the sample, to examine the reproducibility of the findings. Elevated OFC response to cues for impending high-calorie beverage tastes predicted weight gain in both halves of the sample, though elevated reward response to high-calorie beverage tastes did not predict weight gain in that larger study (Stice et al., 2015). We recruited initially health weight adolescents for that study to reduce the possibility that a history of overeating altered neural responsivity. Thus, four studies provide evidence that individuals who show elevated reward region responsivity to food images and cues show greater future weight gain. The fact that somewhat different reward regions were implicated in these studies may have resulted because the studies used different fMRI paradigms and examined different populations. Elevated reward region response to tastes of high-calorie beverages emerged in only one of three studies, and that study had the smallest sample (n = 16). Collectively, results are consistent with the incentive sensitization model, which posits that cues that are repeatedly associated with palatable food intake come to activate reward regions and that this elevated reward region responsivity to food cues prompts overeating (Berridge et al., 2010).

There is also evidence that the *TaqIA* polymorphism (rs1800497) moderates these predictive effects. Elevated dorsal striatum response to high-calorie beverage tastes, cues for impending high-calorie beverage tastes, and high-calorie images predicted future weight gain for adolescents with a genetic propensity for greater DA signaling due to possessing the A2/A2 allele, whereas lower dorsal striatum response to these three events predicted future weight gain for adolescents with a genetic propensity for lower DA signaling due to possessing an A1 allele (Stice et al., 2008a, 2010, 2015). Humans with the A2/A2 variant have 30–40% more DA D2 receptors and greater reward region responsivity versus those with the A1/A1 or A1/A2 variants (Bowirrat & Oscar-Berman, 2005). Results suggest a non-linear relation,

wherein individuals with very high or low DA signaling in reward circuitry may both be at risk for overeating (Stice et al., 2015).

We sought to provide a second sensitive test of the relation of neural responsivity to high-calorie beverage tastes and images to future weight gain, and the moderating effects of the *TaqIA* polymorphism, by collecting data from 135 healthy weight adolescents (again, to rule out the possibility that a history of overeating contributed to aberrant responsivity). Further, because animal models suggest that sugar and fat composition of palatable food imparts differential motivation to eat and gain weight (Avena et al., 2009), we examined the effects of neural responses to beverages varying in fat and sugar content on future weight gain. We also used a novel bootstrapping sampling approach to evaluate whether results that emerge from whole-brain analyses are reliable in response to concerns about the replicability of neuroimaging findings (Szucs & Ioannidis, 2017).

2. Materials and Methods

2.1 Participants

135 adolescents (73 female, 62 male; mean age = 15.0 ± 0.9; mean body mass index (BMI)= 21.2 ± 2.2) were recruited in a US city (Portland, Oregon) via advertisements for a 3-year prospective study. Participants reported the following racial and ethnic backgrounds: 9% Hispanic, 3% American Indian/Alaska Native, 6% Asian, 12% African-American, 2% Pacific Islander, 78% European-American. Individuals who had a reported BMI < 18 or > 25, reported binge eating or compensatory behavior in the past 3 months, any current use of psychotropic medications or illicit drugs or Axis I psychiatric disorder in the past year were excluded. Participants provided assent and parents provided written informed consent for this Oregon Research Institute Institutional Review Board approved study. This project was registered at clinicaltrials.gov before data collection began (NCT01949636).

2.2 Experimental Design

2.2.1 fMRI food receipt paradigm.—Participants completed a food receipt paradigm and a food picture paradigm. The food receipt paradigm was designed to determine whether sugar or fat was more effective in recruiting reward circuitry (Stice et al., 2013). It assessed response to tastes of 4 chocolate milkshakes varying in sugar and fat content and a tasteless solution. Participants were told that they would receive 4 different kinds of milkshake but were not informed about the fat and sugar content of the milkshakes. Each milkshake included the same ice cream base and chocolate syrup. No fat substitutes/thickeners or artificial sweeteners were used. Fat content of the milkshakes was manipulated by varying the milk type (half and half versus 2% milk). Sweetness was manipulated by varying simple syrup content. The task involved receiving tastes of the following milkshakes: a high-fat/high-sugar milkshake (170 kcal, 7.5g fat, and 23 g sugar/100 mL), a high-fat/low-sugar milkshake (129 kcal, 9.0g fat, and 7.3g sugar/100 mL), a low-fat/high-sugar milkshake (124 kcal, 1.9 g fat, 23.7 g sugar/100 mL), and a low-fat/low-sugar milkshake (74 kcal, 2.4g fat, and 8.7 g sugar/100 mL). Pictures of glasses of milkshake or water were presented (1 sec) to cue the participant that they were about to receive milkshake or tasteless solution. All milkshakes were preceded by the same image of a milkshake to not confound the neural

response to tastes with expectations. During milkshake and tasteless solution delivery, a fixation cross was shown. Participants were instructed to hold the taste in their mouth until they saw the 'swallow' cue on the screen, which followed after each taste. Delivery of the milkshake and tasteless solution occurred in variable-length blocks (1 block presented 4, 5, or 7 events in each of the 2 runs) to add an element of unpredictability. Only one type of milkshake was delivered per block. An event was considered when a tastant was delivered (0.7 cc) over 5 secs. After a block was completed, subjects received a rinse of the tasteless solution followed by a swallow cue (0.5 sec) and a jitter (9–11 secs). The tasteless solution followed the same pattern without a rinse. The order of the presentation of blocks (i.e., different milkshakes) was randomized. Two runs (13 min each) were performed. Each run presented 3 blocks of each of the 4 milkshake types and the tasteless solution in random order. There were 6 blocks of each of the 5 tastants. Tastes of these chocolate milkshakes in this paradigm activated brain regions implicated in reward (caudate, putamen), attention (anterior cingulate cortex), and gustatory processing (insula, Rolandic operculum; main effects and significant differences in BOLD response to and pleasantness ratings of the tastes were reported previously for the first 106 participants recruited for the present study (Stice, Burger, & Yokum, 2013).

2.2.2   fMRI food picture paradigm.—The food picture paradigm was designed to examine brain responses to imagined consumption of appetizing foods, unappetizing foods, and glasses of water shown in pictures. Prior to scanning, participants rated how appetizing in general they found foods shown in 129 pictures using a visual analog scale (range: "least appetizing" = −395 to "most appetizing"= 395). Food pictures included processed foods (e.g., cupcakes), fruits (e.g., peaches), and vegetables (e.g., cauliflower). Participants were instructed to use a "YUCK" button if they had a strong aversion to the food (such food images were excluded from the MRI scan and analyses). During the food image paradigm, each participant was exposed to the 32 pictures of food they rated as the most appetizing and the 32 pictures of food they rated as least appetizing, to tailor the pictures to individual preferences, as well as 32 pictures of water. We used glasses of water as a contrast because people drink water daily and water contains no calories. The images were presented for 5 secs. Participants were asked to imagine tasting and eating the pictured food or water. Trials were separated by a fixation cross, presented for 2 to 4 secs. Order of presentation was random. High-calorie food pictures activate brain regions implicated in reward (striatum, medial OFC, mid insula), attention (precuneus, superior parietal lobe, anterior cingulate cortex), motor approach (supplemental motor area) and somatosensory processing (postcentral gyrus, Rolandic operculum) (Stice et al., 2010; Van Meer et al., 2015). It is important to note that tailoring the food images to the individual participant preferences irrespective of caloric content has not been done previously. Fortuitously, the energy density of the foods rated as the most and the least appetizing did not significantly differ ($t = 1.58$, $p = 0.12$; Sadler et al., 2018), which allowed us for the first time to examine the effect of exposure to appetizing versus unappetizing food images that was not confounded by differences in caloric density. Appetizing food pictures in this paradigm resulted in robust activation in brain regions implicated in reward (striatum, medial OFC, mid insula), attention (precuneus, superior parietal lobe, anterior cingulate cortex), motor approach

(supplemental motor area), and somatosensory processing (Rolandic operculum) (see Table 1 for all significant main effect peaks).

2.3 Measures

2.3.1 Body Mass Index.—The body mass index (BMI = kg/m^2) was used to reflect adiposity. Height was measured to the nearest millimeter and weight was assessed to the nearest 0.1 kg (after removal of shoes and coats) at baseline and at 1-, 2-, and 3-year follow-up. BMI correlates with direct measures of total body fat such as dual energy X-ray absorptiometry ($r = 0.80$ to 0.90) and with health measures including blood pressure, adverse lipoprotein profiles, atherosclerotic lesions, serum insulin levels, and diabetes mellitus in adolescent samples (Dietz & Robinson, 1998; Steinberger et al., 2006). Raw BMI scores are superior to age-and sex-adjusted percentiles or BMI z-scores for modeling change over time in longitudinal analyses (Berkey & Colditz, 2007).

2.3.2 Hunger.—Participants were asked to consume their regular meals but to refrain from eating or drinking (other than water) for 4 hours immediately preceding their scan for standardization of hunger and to emulate the hunger exhibited by most people when they approach their next meal, as described in (Stice et al., 2013). Scans typically occurred in the late mornings or late afternoons about 4 hours after typical meal times. Hunger ratings were assessed on 20-cm cross-modal visual analog scales (VASs) immediately before the MRI scan. VAS ratings were anchored by −10 (not at all), 0 (neutral), and 10 (never been more hungry). The mean (±SD) hunger rating was 0.8 ± 4.3, suggesting that participants were on average in a neutral hunger state (given that one might have expected them to be more hungry after not eating for 4 hours, this may suggest some problems with compliance).

2.3.3 Taste ratings.—For hedonic ratings, participants sampled a small amount of each milkshake and the tasteless solution (order counterbalanced) and rated the pleasantness on a scale ranging from 0 (most unpleasant sensation ever) to 20 (most pleasant sensation ever). Pleasantness ratings (Table 2) varied significantly between the 4 milkshakes and tasteless solution (Table 2), with the exception of ratings of low-fat/low-sugar milkshake compared with the tasteless solution (P = 0.10). The high-fat/high-sugar milkshake, high-fat/low-sugar milkshake, and low-fat/high-sugar milkshake were all rated as significantly more pleasant than the tasteless solution.

2.3.4 Dietary restraint.—The Dutch Eating Behavior Questionnaire (DEBQ) is a 33-item inventory assessing several key factors of eating behavior including restraint eating, external eating and emotional eating (van Strien et al., 1986). The restrained eating subscale scale assesses dietary behaviors designed to produce weight loss and weight maintenance on a Likert-scale, with scores ranging from 1 to 5. This scale has shown internal consistency (α's range from .93 to .95) and temporal reliability; 2-week test-retest r = .82 (Stice, et al., 2004; van Strien et al., 1986). Although this scale correlated with self-reported caloric intake (French, et al., 1994; Laessle, et al., 1989) it did not correlate with objectively measured caloric intake (Stice, et al., 2004; Stice, et al., 2010a).

2.3.5   Impulsivity.—The Barratt Impulsivity Scale (BIS-11) was used to assess trait impulsivity (Patton, Stanford, & Barrett, 1995). This scale has shown internal consistency (α = .79 –.83), 2-week test-retest reliability (r = .88), and discriminates between psychiatric patients and controls (Patton et al., 1995; Suris et al., 2004). We assessed dietary restraint and impulsivity to aid in the interpretation of significant BOLD peaks.

2.3.6   TaqIA rs1800497 genotyping.—Participants were asked to provide saliva, from which epithelial cells were collected, using a commercial product (Oragene, DNA Genotek Inc, Ottawa, Ont). DNA was extracted from saliva using standard salting-out and solvent precipitation methods, yielding an average of 4 μg of DNA. The genotype was determined using the Taqman allelic discrimination assay (ThermoFisher Scientific, Waltham, MA) to query the polymorphism. Assays were done using a fluorogenic 5' nuclease method on a StepOne Plus quantitive PCR instrument (Applied Biosystems Inc, Foster City, CA). Reactions contained 10 ng of DNA in a volume of 10 ul, which were amplified using the TaqMan Genotyping Master Mix and the standard cycling conditions. The amplification primers and probes are commercially available (Assay ID C_30090620_10), pre-labeled with VIC/FAM dyes and quenched with MGB/NFQ. Each 96-well plate included non-templates, DNA standards of known genotype, and 10% sample replication for accuracy. Concordance between replicates was 100%. Fifteen of the 135 participants did not provide a saliva sample and were excluded from the analyses involving *TaqIA*. The following *TaqIA* groups were defined: A1/A1 variant (n = 7), A1/A2 variant (n = 46), and A2/A2 variant (n = 64).

2.4   Statistical analysis

2.4.1   Change in BMI.—BMI data from baseline, and 1-, 2-, and 3-year follow-ups were used in random intercept, mixed effects growth curve analyses (SAS Inc. version 9.3) to model BMI change. Following Singer and Willet (2003), we: (1) examined empirical growth plots; (2) fit an unconditional means model; (3) fit an unconditional linear growth model; and (4) fit unconditional nonlinear models. We compared the latter two models using the Akaike information criterion (AIC) to determine whether linear or higher-order polynomial models fit the data better. AIC is a measure of goodness of fit relative to model complexity (Burnham & Anderson, 2002). Compared with higher-level polynomial models, linear growth models consistently showed a better fit per AIC values, suggesting that linear terms optimally captured change in body fat.

2.4.2   fMRI data acquisition.—MRI data were acquired on a Siemens Tim Trio 3 Tesla MRI scanner. BOLD echo-planar images (BOLD-EPI) were acquired with T2* -weighted gradient echo sequence (TE = 30 ms, TR = 2000 ms, flip angle = 80º) with an in-plane resolution of 3.0×3.0 mm2 (64×64 matrix; 192×192mm2 field of view). To cover the whole brain, 32 slices, 4mm (interleaved acquisition, no skip), were acquired along the AC-PC transverse, oblique plane as determined by the midsagittal section. Structural scans were collected using an inversion recovery T1-weighted sequence (MP-RAGE) in the same orientation as the functional sequences to provide detailed anatomic images aligned to the functional scans. High-resolution structural MRI sequences (FOV = 256×256 mm^2, 256×256 matrix, thickness = 1.0 mm, slice number = 160) were acquired. fMRI data of 3

participants were collected with an acquisition error and therefore excluded from analyses. Prospective acquisition correction (PACE) was used to adjust slice position and orientation, as well as to re-grid residual volume-to-volume motion in real-time during data acquisition for the purpose of reducing motion-induced effects (Thesen et al., 2000). No participant's data failed to meet the movement inclusion criteria, which were that within-run movement before correction did not exceed 2 mm in translational movement and 20 in rotational movement. For smaller movements, PACE adjusts slice position, orientation and re-grids the residual volume-to-volume motion during data acquisition.

2.4.3   fMRI data preprocessing.—DICOM images were converted to NIfTI format via MRIConvert (http://lcni.uoregon.edu/~jolinda/MRIConvert/). Before preprocessing, images were manually realigned to the AC-PC line in SPM and skull-stripped using the Brain Extraction Tool in FSL (FMRIB Analysis Group, Oxford, UK). During preprocessing in SPM, anatomical data were segmented and normalized using DARTEL, resulting in a sample-specific template and individual-level deformation fields for application to the normalization step during functional data preprocessing. Functional data were preprocessed as follows: (1) slice timing corrected; (2) adjusted for variation in magnetic field distortion using field maps (Poldrack et al., 2011); (3) realigned to the mean functional from that run and coregistered with the anatomical; and (4) normalized to Montreal Neurological Institute (MNI) space using the DARTEL template and deformation fields output, which allows more precise alignment (Klein et al., 2009). Functional data were smoothed to 6 mm Gaussian full-width-at-half-maximum (FWHM) and then assessed to detect spikes in global mean response and motion outliers in the functional data using the Artifact Detection Toolbox (ART; Gabrieli Laboratory, McGovern Institute for Brain Research, Cambridge MA). Motion parameters were included as regressors in the design matrix at individual-level analysis. Additionally, image volumes where the z-normalized global brain activation exceeded 3 SDs from the mean of the run or showed >1 mm of composite (linear plus rotational) movement were flagged as outliers and de-weighted during individual-level model estimation. Activation in response to the intake of each milkshake was assessed by contrasting BOLD signal during receipt of each of the 4 milkshakes versus tasteless solution. Because there were significant differences in BOLD response to and pleasantness ratings of the 4 milkshakes (Stice et al., 2013), we decided not to collapse the data across all 4 milkshakes as this would have introduced noise. However, because pleasantness ratings did not significantly differ between the low-fat/low-sugar milkshake and tasteless solution (Table 2) and because there were also no significant differences in BOLD activation in the mesolimbic circuitry between these two tastes (Stice et al., 2013), this contrast was excluded from the analyses. To identify brain regions activated in response appetizing food images, we contrasted BOLD signal during viewing pictures of appetizing food versus unappetizing foods and during viewing pictures of appetizing food pictures versus glasses of water. Individual maps were constructed to compare the activations within each participant for these 5 contrasts.

2.4.4   fMRI data analysis.—To test whether BOLD response to milkshake tastes and appetizing food pictures predicted BMI gain, individual SPM contrasts were entered into a second-level regression model with BMI slopes and intercepts as covariates (see below).

Hunger (all models) and pleasantness ratings (milkshake taste models) were included as a covariate of no interest. Whole-brain analyses were conducted after the binarized DARTEL-derived sample-specific gray matter mask was applied. An overall significance level of $p<0.05$ corrected for multiple comparisons across the gray matter-masked whole brain was calculated. This was accomplished by first estimating the intrinsic smoothness of the masked functional data with the spatial autocorrelation function (acf) option in the three-dimensional FWHM module in AFNI (Version AFNI_17.0.03). The acf parameters were then used in 10,000 Monte Carlo simulations of random noise at 3 mm^3 through the gray matter masked data with the 3DClustSim module of AFNI. Simulation results indicated activity surviving a threshold of $p<0.001$, with a cluster (k)   37 being statistically significant corrected for multiple comparisons.

There has been increasing concern regarding the reliability of findings from brain imaging studies, primarily due to use of small samples, which increases the leverage of influential outliers that drive chance findings, and liberal statistical significance thresholding (Button et al., 2013; Cremers et al., 2017). In response to the former issue, we have recruited larger samples than are typically employed in neuroimaging studies. In response to the latter issue, we have used split-half replication to increase the likelihood that the effects are replicable (Stice et al., 2015). Yet split-half replication may not be optimal because using only half the sample size reduces sensitivity, increasing risk for false negative findings. Accordingly, we used a novel bootstrapping replication approach wherein we randomly selected 80% of the sample (without replacement) 10 times and tested whether BOLD response to the 5 events of interest predicted elevated future BMI gain in each sample. We decided to randomly select 80% of the total sample to ensure reasonable sensitivity, in that each sample contained data from just over 100 participants. We decided to draw 10 bootstrap samples because we thought this would be sufficient for determining if particular effects generally emerged in the bootstrap samples. Effects that emerge in whole-brain analyses with the full sample and replicated in each of the 10 samples should be more likely to replicate in future studies. To test whether the bootstrapping replication approach is more sensitive than the split-half replication approach, we also conducted split-half analyses with the present data.

In an effort to replicate the effects from previous independent prospective fMRI studies (Demos et al., 2012; Geha et al., 2013; Stice et al., 2008a,b; Yokum et al., 2014), we performed *a priori* small volume correction (SVC) analyses within the striatum, ventral pallidum, hypothalamus, thalamus, and midbrain with activation peaks from these studies as centroids to define 10-mm diameter spheres. It is important to acknowledge that the paradigms we used in the present study were somewhat different than used in these previous studies (meaning these were not direct replication tests). Peaks within these regions were considered significant at $p<0.05$, familywise error rate (FWE) corrected over the 10 mm sphere. To test whether *TaqIA* moderated the relation of neural response and future BMI gain, we conducted multiple regression models using SPSS. Independent variables included BMI intercept, *TaqIA*, neural response, and the interaction between *TaqIA* and neural response. For these analyses we extracted mean activity (parameter estimates) of significant peaks in response to the food receipt and food image paradigms using MarsBar (http://www.marsbar.source-forge.net) and exported the data to SPSS. We also extracted mean activity within the striatum using peaks from previous prospective fMRI studies which found

that *TaqIA* moderated the relation between neural response in the striatum and BMI gain as centroids to define 10-mm diameter spheres (Stice et al., 2008a, 2010, 2015). Mean activity from these SVC analyses was exported to SPSS. All data were visually inspected to ensure that influential outliers did not drive effects.

We estimated effect sizes (*r*) based on the reported *Z*-values and sample size using a formula from Rosenthal (1991) because methodologists recommend reporting and interpreting effect sizes with fMRI data (Cremers et al., 2017; Soares et al., 2016).

3. Results

Table 3 presents information about annual BMIs throughout the study period. From baseline to 3-year follow-up, 41% of the sample showed increases in BMI (n = 55); 11.3% of the sample became overweight or obese over follow-up (n = 15). Participants rated appetizing food images (mean = 308.7 ± 69.6) significantly as more appetizing than unappetizing food images (mean = −244.6 ± 122.0): mean difference = 32.07 ± 64.0; *t*[130] = 41.7, *P* < 0.001). On average, individuals reported low dietary restraint (M = 1.67 ± .64) and general impulsivity (M = 1.02 ± 0.28).

3.1 Relations of baseline BOLD activity to milkshake tastes and BMI gain over 3-year follow-up

Lower BOLD response in the left pre-supplementary motor area (pre-SMA r = −0.42; Fig 1) to the high-fat/low-sugar milkshake receipt > tasteless solution receipt contrast predicted BMI gain over 3-year follow-up (Table 4). The observed effect of neural activation in the pre-SMA on BMI gain was statistically significant in 5 of the 10 random bootstrap subsamples (50%), which each included 80% of the cases (Table 5, Fig 2), but was not significant in either of the split-halves of the sample. The pre-SMA has been implicated in inhibitory processes (for meta-analyses, see Simmonds et al., 2008, Swick et al., 2011, Criaud & Boulinguez, 2013), including to food stimuli (Hollman et al., 2012; Van der Laan et al., 2014). Therefore, we conducted post-hoc analyses testing whether the significant effects in the pre-SMA to the high-fat/low-sugar milkshake receipt > tasteless solution receipt contrast correlated with the Dutch Restraint Eating Scale and with the Barratt Impulsiveness Scale. For these analyses we extracted mean activity (parameter estimates) of the significant peaks in the pre-SMA and exported the data to SPSS. We found a significant correlation between activity within the pre-SMA with dietary restraint (*r* = 0.23, p <0.01), but not with general impulsivity (r = −0.06, p = 0.53). There were no significant associations between BOLD response to high-fat/high-sugar milkshake receipt > tasteless solution receipt and low-fat/high-sugar milkshake receipt > tasteless solution receipt contrasts and BMI gain over follow-up. Similar analyses were done with standardized BMI scores (BMI z-scores). The average BMI z-score slope was −0.11 ± .43. There were no significant associations between the events of interest and zBMI gain over follow-up.

We performed region-of-interest searches using peaks in the nucleus accumbens, ventral pallidum, hypothalamus, anterior thalamus, midbrain, precuneus, and superior parietal lobe identified previously in response milkshake receipt (Geha et al., 2013; Stice et al., 2015) as centroids to define 10-mm diameter spheres. None of these *a priori* regions of interest in

response to any of the 3 milkshake taste contrasts were significantly related to future BMI gain in the present sample.

3.2 Relation of baseline BOLD activity to appetizing food pictures and BMI gain over 3-year follow-up

Elevated BOLD response in the left precentral gyrus ($r = 0.41$; extending into the left Rolandic operculum [$r = 0.31$]; Fig 3) to the appetizing food pictures > glasses of water contrast and lower BOLD response in the ventral medial prefrontal cortex (vmPFC $r = -0.35$; extending into the medial orbitofrontal cortex [mOFC $r = -0.33$]) to the appetizing food pictures > unappetizing food pictures contrast predicted BMI gain over 3-year follow-up (Table 4). The associations of the peak voxels and BMI gain in the 10 bootstrap subsamples was as follows: left precentral gyrus: 40% (significant in 4 of the 10 subsamples), vmPFC: 10% (significant in 1 of the 10 subsamples) (Table 5). The observed effects in the precentral gyrus and vmPFC were not significant in either subsample in the split-half analyses. There were no significant associations between BOLD activity in response to the contrasts appetizing food pictures > glasses of water and appetizing food pictures > unappetizing food pictures and zBMI gain over follow-up.

We performed region-of-interest searches using peaks identified previously in response to food images/cues, namely the striatum (Demos et al., 2012; Yokum et al., 2014) and lateral OFC (Stice et al., 2015) as centroids to define 10-mm diameter spheres. None of the peaks were significantly related to BMI gain in the present sample.

3.3 Moderating effects of TaqIA on the relations of baseline BOLD responsivity to milkshake tastes and appetizing food pictures to BMI gain over 3-year follow-up

X^2 analyses indicated that there were no significant relations between genotype status and reported ethnicity, race, or sex, suggesting that ancestry and sex are not potential confounds. X^2 analyses also indicated that the *TaqIA* gene is in Hardy-Weinberg equilibrium ($X^2 = 0.08$). *TaqIA* moderated the association of BOLD activity in the left pre-SMA in response to the high-fat/low-sugar milkshake receipt > tasteless solution contrast and BMI gain. The interactive effects suggest that lower pre-SMA activation in response to high-fat/low-sugar milkshake receipt vs tasteless solution receipt predicted greater BMI gain more strongly in A1 carriers ($r = -0.53$, $p<0.001$) than in A2/A2 carriers ($r = -0.36$, $p<0.01$) (Fig 4). *TaqIA* did not moderate any of the associations between the other peaks and BMI gain. There was also no significant interaction effect of *TaqIA* and striatum activity per region of interest in response to the various contrasts in the milkshake receipt and food picture tasks on BMI gain.

4. Discussion

Whole-brain analyses indicated that lower response in the pre-supplemental motor area to high-fat/low-sugar milkshake taste predicted elevated future BMI gain in the full sample. This effect emerged in 5 out of the 10 bootstrap samples, suggesting that this peak is only a moderately reliable effect. The pre-SMA is implicated in various motor processing functions, such as motor inhibitory processes (for meta-analyses, see Simmonds et al., 2008,

Swick et al., 2011, Criaud & Boulinguez, 2013), including to food stimuli (Hollman et al., 2012; Van der Laan et al., 2014) and motor imagery (Mackary et al., 2017). Further, obese versus healthy weight individuals show less activation in this region during cognitive appetite control (Tuulari et al. 2015). Activation in the pre-SMA correlated positively with dietary restraint, but not with general impulsivity. Therefore, these results might be interpreted as providing evidence that individuals with lower motor inhibitory control in response to palatable food tastes are less able to regulate their desire for these foods, increasing risk for overeating and weight gain, consistent with the inhibitory control deficit model of obesity (Nederkoorn et al., 2006). As such, the pre-SMA finding converges with evidence that inhibitory control deficits in response to high-calorie foods in delay discounting tasks, which reflects an immediate reward bias, has reliably predicted future weight gain (Evans et al., 2012; Francis & Susman, 2009; Schlam et al., 2013; Seeyave et al., 2009). The pre-SMA finding also converges with evidence that participants who showed less recruitment of inhibitory control regions (inferior, middle, and superior frontal gyri) during difficult versus easy choices on a delay-discounting task showed elevated future weight gain ($r = .71$; Kishinevsky et al., 2012) and with evidence that individuals that showed less recruitment of inhibitory control regions (dorsolateral prefrontal cortex) during a delay discounting task showed significantly less weight loss in response to weight loss treatment (Weygandt et al., 2013) and less weight loss maintenance over a 1-year follow-up (Weygandt et al., 2015). However, it is not reassuring that low pre-SMA response to the tastes of the other two types of milkshake did not predict future weight gain.

Higher response in the precentral gyrus, extending into the Rolandic operculum, to appetizing food images also predicted BMI gain in the full sample. This effect emerged in only 4 out of the 10 bootstrap samples, suggesting that this effect is not very reliable. The precentral gyrus is a motor processing region and involved in motor coordination and planning. Obese versus healthy weight individuals show greater activation in this region in response to food versus nonfood images (see for meta-analysis; Brooks et al., 2013). Increased activation in this region in response to palatable food images has been interpreted as reflecting motor planning about ingesting such foods (Geliebter et al., 2006). The Rolandic operculum is an oral somatosensory region that is associated with sensation in the mouth, lips, and tongue (Wang et al., 2002). Obese versus lean individuals show greater activation in the Rolandic operculum in response to pictures of high-calorie foods versus low-calorie foods and control images (Dimitropoulos et al., 2012; Martin et al., 2010; Stoeckel et al., 2008; Stice et al., 2010) and cues predicting impending palatable food receipt (Stice et al., 2008b). Thus, results may suggest that individuals who show elevated motor planning and anticipation of oral somatosensory stimulation from imagined intake of the pictured appetizing foods may be at elevated risk for overeating and weight gain, though this interpretation is based on reverse inference. More importantly, the fact that this relation emerged in only 4 out of the 10 bootstrap samples suggests that it is not very reliable. Further, the fact that response of the precentral gyrus/Rolandic operculum to appetizing pictures versus unappetizing pictures, or to milkshake tastes, did not predict future weight gain does not inspire confidence in this effect either.

Lower response in the ventromedial prefrontal cortex to appetizing food images also predicted BMI gain in the full sample. The vmPFC plays a critical role in evaluating

rewarding stimuli (O'Hare et al., 2009; Plassmann et al., 2010) and has been found to be more active during exposure to food relative to neutral stimuli (Killgore et al., 2003). Martin et al. (2010) found that obese versus lean children showed *greater* response in the vmPFC to food images. Strikingly, this peak only replicated in 1 of the 10 bootstrap samples, implying it is not a reliable effect. Thus, the present study found little reliable evidence that elevated responsivity of regions implicated in reward to appetizing food images predicted future weight gain, as observed in some previous studies (Demos et al., 2012; Yokum et al., 2014), though not in others (Stice et al., 2010). Although the present results suggest that the previously reported effects might be unreliable, potentially due to the use of smaller samples, it is important to note that the food images rated as the most and least appetizing that were used in the contrast in the present study had similar caloric density. Palatability is often confounded with caloric density of images of food, which complicates interpretation. Thus, it is possible that the previously reported effects were due to differences in caloric density rather than with regard to whether the foods were appetizing versus unappetizing. A previous study found that caloric density correlated positively with neural response to food pictures in regions implicated in reward (Tang et al., 2013). It might therefore be best for future studies to focus on neural responsivity to high-calorie food images. Another factor that might explain the non-replication is that all of our participants were in a healthy weight range at baseline, to rule out the possibility that a history of overeating altered neural responsivity. Although one previous study likewise focused on healthy weight adolescents for the same reason (Stice et al., 2015), and found that elevated OFC response to anticipated milkshake tastes predicted future weight gain, other studies that reported predictive effects included overweight and obese participants (Demos et al., 2012; Geha et al., 2013; Yokum et al., 2011, 2014), raising the possibility that a history of overeating contributed to the aberrant neural responsivity that predicted future weight gain.

It was also noteworthy that there was no evidence that elevated responsivity of regions implicated in reward to high-calorie milkshake receipt predicted future weight gain. On the one hand, these findings converge with the results of two past studies (Stice et al., 2008a, 2015). On the other hand, one study found that elevated responsivity of regions implicated in reward processing predicted future weight gain, though that study used a very small sample (n = 16; Geha et al., 2013). Interestingly, two studies have found that healthy weight adolescents at high risk for future weight gain by virtue of parental obesity showed elevated reward region response to receipt of high-calorie beverages (Shearrer, Stice, & Burger, 2018; Stice et al., 2011). Collectively, the pattern of findings provide little reliable support for the thesis that elevated responsivity of regions implicated in reward to high-calorie food receipt increases risk for future weight gain (Davis et al., 2004). It could be argued that we did not observe elevated responsivity of reward regions to milkshake receipt because participants were always cued that they were going to receive a taste of milkshake. Research has found that reward region response to palatable food tastes is weaker when anticipated versus when not anticipated (Steinberg et al., 2013). However, as noted in the methods section, main effects analyses confirmed that the tastes of chocolate milkshake in our paradigm activated striatal regions, such as the caudate and putamen (Stice et al., 2013), even when consistently cued.

Further, ROI analyses did not replicate the predictive effects of peaks reported previously (Demos et al., 2012; Yokum et al., 2014). In addition, there was no evidence that the *TaqIA* polymorphism moderated any of the predictive effects reported in previous reports (Stice et al., 2008a, 2010, 2015). However, it is important to acknowledge that the paradigms we used in the present study differed from those used in these earlier studies. Therefore these null findings should not be considered as a direct replication test of earlier findings.

Finally, we used a novel bootstrap sampling approach to evaluate the reliability of the effects observed in the full-sample analyses. This approach appears to be useful in determining whether the observed whole sample effects are reliable. Further, the bootstrapping approach was more sensitive than split-half analyses, which did not identify a single effect that replicated in both halves of the sample. Thus, it might be useful for future studies to use large samples and conduct such reliability testing in bootstrap subsamples, as this approach should allow identification of effects that are more reliable versus those that are less reliable. The fact that it was so difficult to identify peaks that emerged in whole-brain analyses in each of the 10 bootstrap samples provides further evidence that fMRI analyses may over-fit models to data, which results in findings that are not reliable (Cremers et al., 2017).

It is important to consider the limitations of this study. First, because we recruited healthy weight adolescents at baseline to reduce the possibility that a history of overeating produced alterations in neural responsivity to food stimuli, this might have made it difficult to predict future increases in BMI. However, it is important to note that we found that family history of obesity did predict future BMI gain over follow-up in this sample (Shearrer et al., 2018), suggesting that we had sufficient sensitivity to detect such predictive effects. Second, it would have been desirable to have followed participants for more than 3-years, as some who did not exhibit excess weight gain in the follow-up period, likely will when they grow older. Third, the paradigm used to examine BOLD response to imagined intake of palatable foods versus glasses of water shown in pictures might have been less than ideal because eating foods is somewhat different than drinking beverages, and further, we did not assess thirst or use thirst ratings as a covariate. It would therefore be preferable to restrict the focus to imagined intake of high-versus low-calorie foods shown in pictures in future studies.

Conclusions and Future Directions for Research

Results suggest that individuals who show lower response in the pre-supplemental motor area to high-fat/low-sugar milkshake taste and elevated response in the precentral gyrus/ Rolandic operculum to imagined intake of appetizing foods may be at elevated risk for excessive weight gain. However, there was little evidence that elevated responsivity of regions implicated in reward to receipt of high-calorie beverages or to appetizing food images predicted future weight gain, or that the *TaqA1* polymorphism moderated such predictive effects, though the lack of convergence with past findings may be due to the fact that our paradigms differed from those used in the past studies. Finally, results suggest that bootstrap sampling may allow the identification of the most reliable effects from whole-brain analyses, but suggest that fMRI analyses may typically over-fit models to data.

Acknowledgments

References

Avena NM, Rada P, Hoebel BG. (2009) Sugar and fat bingeing have notable differences in addictive-like behavior. J Nutr 139: 623–628. [PubMed: 19176748]

Berridge KC, Ho CY, Richard JM, DiFeliceantonio AG (2010) The tempted brain eats: pleasure and desire circuits in obesity and eating disorders. Brain Res 1350: 43–64. [PubMed: 20388498]

Berkey CS, Colditz GA (2007) Adiposity in adolescents: change in actual BMI works better than change in BMI z score for longitudinal studies. Ann Epidemiol 17: 44–50. [PubMed: 17140812]

Bowirrat A, Oscar-Berman M (2005) Relationship between dopaminergic neurotransmission, alcoholism, and Reward Deficiency syndrome. Am J Med Genet B Neuropsychiatr Genet 132B: 29–37. [PubMed: 15457501]

Brooks SJ, Cedernaes J, Schiöth HB (2013) Increased prefrontal and parahippocampal activation with reduced dorsolateral prefrontal and insular cortex activation to food images in obesity: A meta-analysis of fMRI studies. PLoS One 8: e60393. [PubMed: 23593210]

Burnham KP, Anderson D (2002) Model selection and multi-model inference: a practical information-theoretic approach New York: Springer.

Button KS, Ioannidis JP, Mokrysz C, Nosek BA, Flint J, Robinson ES, Munafo MR (2013) Power failure: why small sample size undermines the reliability of neuroscience. Nat Rev Neurosci 14:365–376. [PubMed: 23571845]

Criaud M, Boulinguez P (2013) Have we been asking the right questions when assessing response inhibition in go/no-go tasks with fMRI? A meta-analysis and critical review. Neurosci Biobehav Rev 37: 11–23. [PubMed: 23164813]

Davis C, Strachan S, Berkson M (2004) Sensitivity to reward: Implications for overeating and overweight. Appetite 42: 131–138. [PubMed: 15010176]

Demos KE, Heatherton TF, Kelley WM (2012) Individual differences in nucleus accumbens activity to food and sexual images predict weight gain and sexual behavior. J Neurosci 32: 5549–5552. [PubMed: 22514316]

Dietz WH, Robinson TN (1998) Use of the body mass index (BMI) as a measure of overweight in children and adolescents. J Pediatr 132: 191–193. [PubMed: 9506622]

Dimitropoulos A, Tkach J, Ho A, Kennedy J (2012) Greater corticolimbic activation to high-calorie food cues after eating in obese vs. normal-weight adults. Appetite 58: 303–312. [PubMed: 22063094]

Cremers HR, Wager TD, Yarkoni T (2017) The relation between statistical power and inference in fMRI. PLoS One 12:e0184923. [PubMed: 29155843]

Evans G, Ruller-Rowell R, Doan S (2012) Childhood cumulative risk and obesity: The mediating role of self-regulatory ability. Pediatrics 129: e68. [PubMed: 22144695]

Ferreira J, Tellez L, Ren X, Yeckel C, de Araujo I (2012) Regulation of fat intake in the absence of flavour signaling. J Physiol 590: 953–972. [PubMed: 22219333]

Francis L, Susman EJ (2009) Self-regulation failure and rapid weight gain in children from age 3 to 12 years. Arch Pediatr Adolesc Med 163: 297–302. [PubMed: 19349557]

Gearhardt AN, Yokum S, Stice E, Harris JL, Brownell KD (2014) Relation of obesity to neural activation in response to food commercials. Soc Cogn Affect Neurosci 9: 932–938. [PubMed: 23576811]

Geha PY, Aschenbrenner K, Felsted J, O'Malley SS, Small DM (2013) Altered hypothalamic response to food in smokers. Am J Clin Nutr 97: 15–22. [PubMed: 23235196]

Geliebter A, Ladell T, Logan M, Schweider T, Sharafi M, Hirsch J (2006) Responsivity to food stimuli in obese and lean binge eaters using functional MRI. Appetite 46: 31–35. [PubMed: 16364498]

Goldstein RZ, Tomasi D, Alia-Klein N, Zhang L, Telang F, Volkow ND (2007) The effect of practice on a sustained attention task in cocaine abusers. NeuroImage 35: 194–206. [PubMed: 17236790]

Hare TA, Camerer CF, Rangel A (2009) Self-control in decision-making involves modulation of the vmPFC valuation system. Science 324: 646–648. [PubMed: 19407204]

Hollmann M, Hellrung L, Pleger B, Schlogl H, Kabisch S, Stumvoll M et al. (2012) Neural correlates of the volitional regulation of the desire for food. Int J Obes 36: 648–655.

Killgore WD, Young AD, Femia LA, Bogorodzki P, Rogowska J, Yurgelun-Todd DA (2003) Cortical and limbic activation during viewing of high-versus low calorie foods. NeuroImage 19: 1381. [PubMed: 12948696]

Kishinevsky F, Cox J, Murdaugh D, Stoeckel L, Cook E, Weller R (2012) fMRI reactivity on a delay discounting task predicts weight gain in obese women. Appetite 58: 582–592. [PubMed: 22166676]

Klein A, Andersson J, Ardekani BA, Ashburner J, Avants B, Chiang MC et al. (2009) Evaluation of 14 nonlinear deformation algorithms applied to human brain MRI registration. NeuroImage 46: 786–802. [PubMed: 19195496]

Makary MM, Eun S, Park K (2017). Greater corticostriatal activation associated with facial motor imagery compared with motor execution: a functional MRI study. Neuroreport 28: 610–617. [PubMed: 28538517]

Martin LE, Holsen LM, Chambers RJ, Bruce AS, Brooks WM, Zarcone JR et al. (2010) Neural mechanisms associated with food motivation in obese and healthy weight adults. Obesity 18: 254–260. [PubMed: 19629052]

Mourao-Miranda J, Volchan E, Moll J, de Oliveira-Souza R, Branati I, Gattass R, Pessoa L (2003) Contributions of stimulus valence and arousal to visual activation during emotional perception. NeuroImage 20: 1955–1963. [PubMed: 14683701]

Mundy ME, Downing PE, Honey RC, Sing KD, Graham KS, Dwyer DM (2014) Brain correlates of experience-dependent changes in stimulus discrimination based on the amount of schedule of exposure. PLoS One 9: e101011. [PubMed: 24967903]

Nederkoorn C, Braet C, Van Eijs Y, Tanghe A, Jansen A (2006). Why obese children cannot resist food: The role of impulsivity. Eati Behav 7: 315–322.

Ouwens M, van Strien T, van der Staak C (2003). Tendency toward overeating and restraint as predictors of food consumption. Appetite 40: 291–298. [PubMed: 12798787]

Patton JH, Stanford MS, Barratt ES (1995). Factor structure of the Barratt impulsiveness scale. J Clin Psychol 51: 768–774. [PubMed: 8778124]

Plassmann H, O'Doherty JP, Rangel A (2010) Appetitive and aversive goal values are encoded in the medial orbitofrontal cortex at the time of decision making. J Neurosci 30: 10799– 10808. [PubMed: 20702709]

Poldrack RA, Mumford JA, Nichols TE (2011) Handbook of fMRI data analysis Cambridge, UK: Cambridge UP.

Rubin DB (1987) Multiple Imputation for Nonresponse in Surveys New York: John Wiley & Sons, Inc.

Sadler J, Shearrer G, Stice E, Burger K (2018) Does adjusting for energy density of preference better characterize brain response to food images? Poster presented at the University of North Carolina This Data Research Conference

Santel S, Baving L, Krauel K, Munte TF, Rotte M (2006) Hunger and satiety in anorexia nervosa: fMRI during cognitive processing of food pictures. Brain Res 1114: 138–148. [PubMed: 16919246]

Schlam TR, Wilson NL, Shoda Y, Mischel W, Ayduk O (2013) Preschoolers' delay of gratification predicts their body mass 30 years later. J Pediatr 162: 90–93. [PubMed: 22906511]

Seeyave D, Coleman S, Appugliese D, Corwyn R, Bradley R, Davidson N, et al. (2009) Ability to delay gratification at age 4 years and risk of overweight at age 11 years. Arch Pediatr Adolesc Med 163: 303–308. [PubMed: 19349558]

Shearrer G, Stice E, & Burger K (2018) Adolescents at high-risk for obesity show greater striatal response to increased sugar content of milkshakes. Am J Clin Nutr 107: 859–866. [PubMed: 29771283]

Simmonds DJ, Pekar JJ, Mostofsky SH (2008) Meta-analysis of Go/No-go tasks demonstrating that fMRI activation associated with response inhibition is task-dependent. Neuropsychologia 46: 224–232. [PubMed: 17850833]

Singer JW, Willet J (2003) Applied longitudinal data analysis: modeling change and event occurrence New York: Oxford UP.

Small DM, Jones-Gotman M, Dagher A (2003) Feeding-induced dopamine release in dorsal striatum correlates with meal pleasantness ratings in healthy human volunteers. NeuroImage 19: 1709–1715. [PubMed: 12948725]

Soares J, Magalhaes R, Moreira P, Sousa A, Ganz E, Sampaio A, et al. (2016). A hitchhiker's guide to functional magnetic resonance imaging. Frontiers in Neuroscience, 10, article 515.

Steinberg E, Keiflin R, Boivin J, Witten I, Deisseroth K, & Janak P (2013). A causal link between pediction errors, dopamine neurons and learning. Nature Neuroscience, 16, 966–973. [PubMed: 23708143]

Steinberger J, Jacobs DR, Raatz S, Moran A, Hong C- P, Sinaiko AR (2006) Comparison of body fatness measurements by BMI and skinfolds vs dual energy X-ray absorptiometry and their relation to cardiovascular risk factors in adolescents. Int J Obes 30: 1170–1170.

Stice E, Burger KS, Yokum S (2013) Relative ability of fat and sugar tastes to activate reward, gustatory and somatosensory regions. Am J Clin Nutr 98: 1377–1384. [PubMed: 24132980]

Stice E, Burger KS, Yokum S (2015) Reward region responsivity predicts future weight gain and moderating effects of the TaqIA allele. J Neurosci 35: 10316–10324. [PubMed: 26180206]

Stice E, Fisher M, Lowe M (2004). Are dietary restraint scales valid measures of acute dietary restriction? Unobtrusive observational data suggest not. Psychol Assess 16: 51–59. [PubMed: 15023092]

Stice E, Spoor S, Bohon C, Small DM (2008a) Relation between obesity and blunted striatal response to food is moderated by TaqIA A1 allele. Science 322: 449–452. [PubMed: 18927395]

Stice E, Spoor S, Bohon C, Veldhuizen MG, Small DM (2008b) Relation of reward from food intake and anticipated food intake to obesity: a functional magnetic resonance imaging study. J Abnorm Psychol 117: 924–935. [PubMed: 19025237]

Stice E, Yokum S, Bohon C, Marti N, Smolen A (2010) Reward circuitry responsivity to food predicts future increases in body mass: moderating effects of DRD2 and DRD4. NeuroImage 50:1618–1625. [PubMed: 20116437]

Stice E, Yokum S, Burger KS, Epstein LH, Small DM (2011) Youth at risk for obesity show greater activation of striatal and somatosensory regions to food. J Neurosci 31: 4360–4366. [PubMed: 21430137]

Stoeckel LE, Weller RE, Cook EW, 3rd, Twieg DB, Knowlton RC, Cox JE (2008) Widespread reward-system activation in obese women in response to pictures of high-calorie foods. NeuroImage 41:636–647. [PubMed: 18413289]

Suris AM, Lind LM, Kashner MT, Bernstein IH, Young K, Worchel J (2005). Aggression and impulsivity instruments: An examination in veterans. Mil Psychol 17: 283–297.

Swick D, Ashley V, Turken U (2011) Are the neural correlates of stopping and not going identical? Quantitative meta-analysis of two response inhibition tasks. NeuroImage 56 1655–1665. [PubMed: 21376819]

Szucs D, Ioannidis JP (2017) Empirical assessment of published effect sizes and power in the recent cognitive neuroscience and psychology literature. PLoS biology 15: e2000797. [PubMed: 28253258]

Tang DW, Fellows LK, Dagher A (2014). Behavioral and neural valuation of foods is driven by implicit knowledge of caloric content. Psych Science 25: 2168–2176.

Thesen S, Heid O, Mueller E, Schad LR (2000) Prospective acquisition correction for headmotion with image-based tracking for real-time fMRI. Magn Reson Med 44:457–65. [PubMed: 10975899]

Tuulari JJ, Karlsson HK Hirvonen J, Salminen P, Nuutila P, Nummenmaa L (2015) Neural circuits for cognitive appetitive control in healthy and obese individuals: An fMRI study. PLoS One 10: e0116640. [PubMed: 25658479]

Turk MW, Yang K, Hravnak M, Sereika SM, Ewing LJ, Burke LE (2009) Randomized clinical trials of weight loss maintenance: a review. J Cardiovasc Nurs 24: 58–80. [PubMed: 19114803]

Van der Laan LN, de Ridder DTD, Viergever MA, Smeets PAM (2014) Activation in inhibitory brain regions during food choice correlates with temptation strength and self-regulatory success in weight-concerned women. Front Neurosci 8: 308. [PubMed: 25324714]

Van Meer F, van der Laan LN, Adan RAH, Viergever MA, Smeets PAM (2015) What you see is what you eat: An ALE meta-analysis of the neural correlates of food viewing in children and adolescents. NeuroImage 104: 35–43. [PubMed: 25285373]

Van Strien T, Frijters J, van Staveren W, Defares P, Deurenberg P (1986). The predictive validity of the Dutch Restrained Eating Scale. Int J Eat Disord 5:747–755.

Wang GJ, Volkow ND, Felder C, Fowler J, Levy A, Pappas N, et al. (2002) Enhanced resting activity of the oral somatosensory cortex in obese subjects. Neuroreport 13: 1151–1155. [PubMed: 12151759]

Weygandt M, Mai K, Dommes E, Leupelt V, Hackmack K, Kahnt T, et al. (2013) The role of neural impulse control mechanisms for dietary success in obesity. NeuroImage 83: 669–678. [PubMed: 23867558]

World Health Organization. Obesity and overweight Fact Sheet 311. Retrieved 11.10.2014 from http://amro.who.int/common/Display.asp?Lang=E&RecID=10203 2013

Yokum S, Gearhardt AN, Harris JL, Brownell KD, Stice E (2014). Individual differences in striatum activity to food commercials predict weight gain in adolescents. Obesity (Silver Spring) 22: 2544–2551. [PubMed: 25155745]

Yokum S, Ng J, Stice E (2011) Attentional bias for food images associated with elevated weight and future weight gain: An fMRI study. Int J Obes 19: 1775–1783.
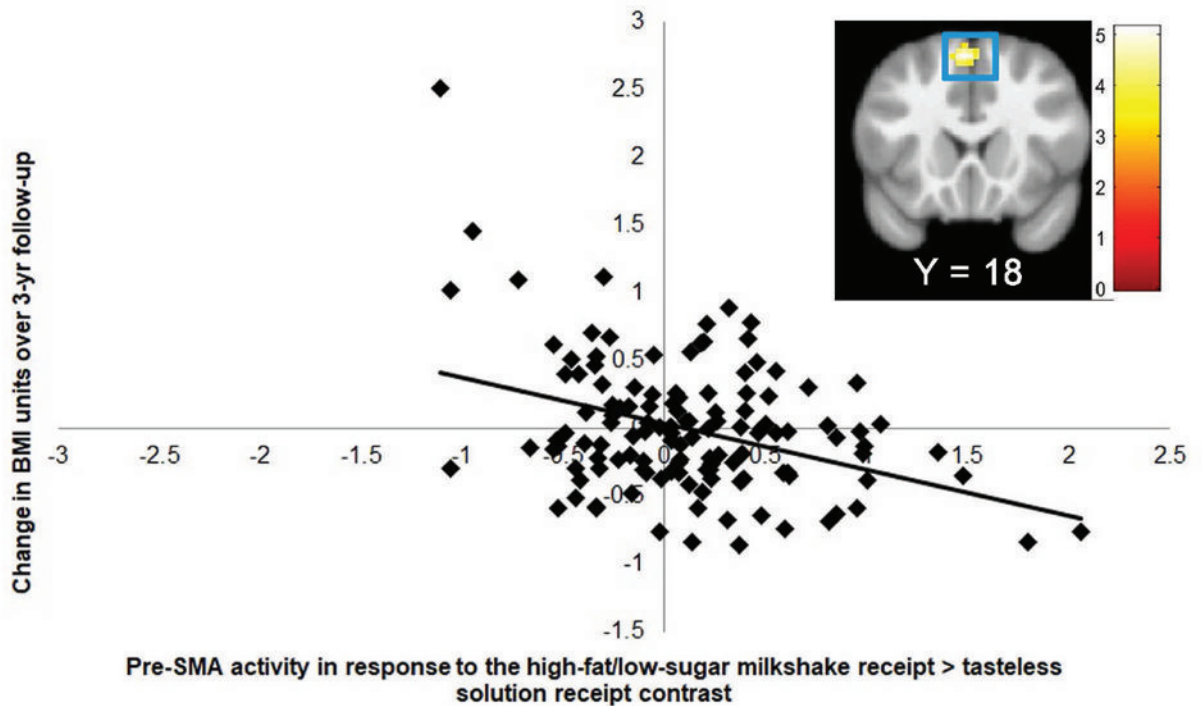
Figure 1.
BOLD activity in the pre-Supplemental Motor Area (pre-SMA; MNI: −3, 18, 54, Z = 4.89, k = 50) to the high-fat/low-sugar milkshake receipt > tasteless solution contrast is negatively associated with BMI gain over 3-year follow-up. The SPM in this figure and all others is threholded at p>0.001; k 32. The color bars represent t-values. The effects remained significant when excluding the outlier.
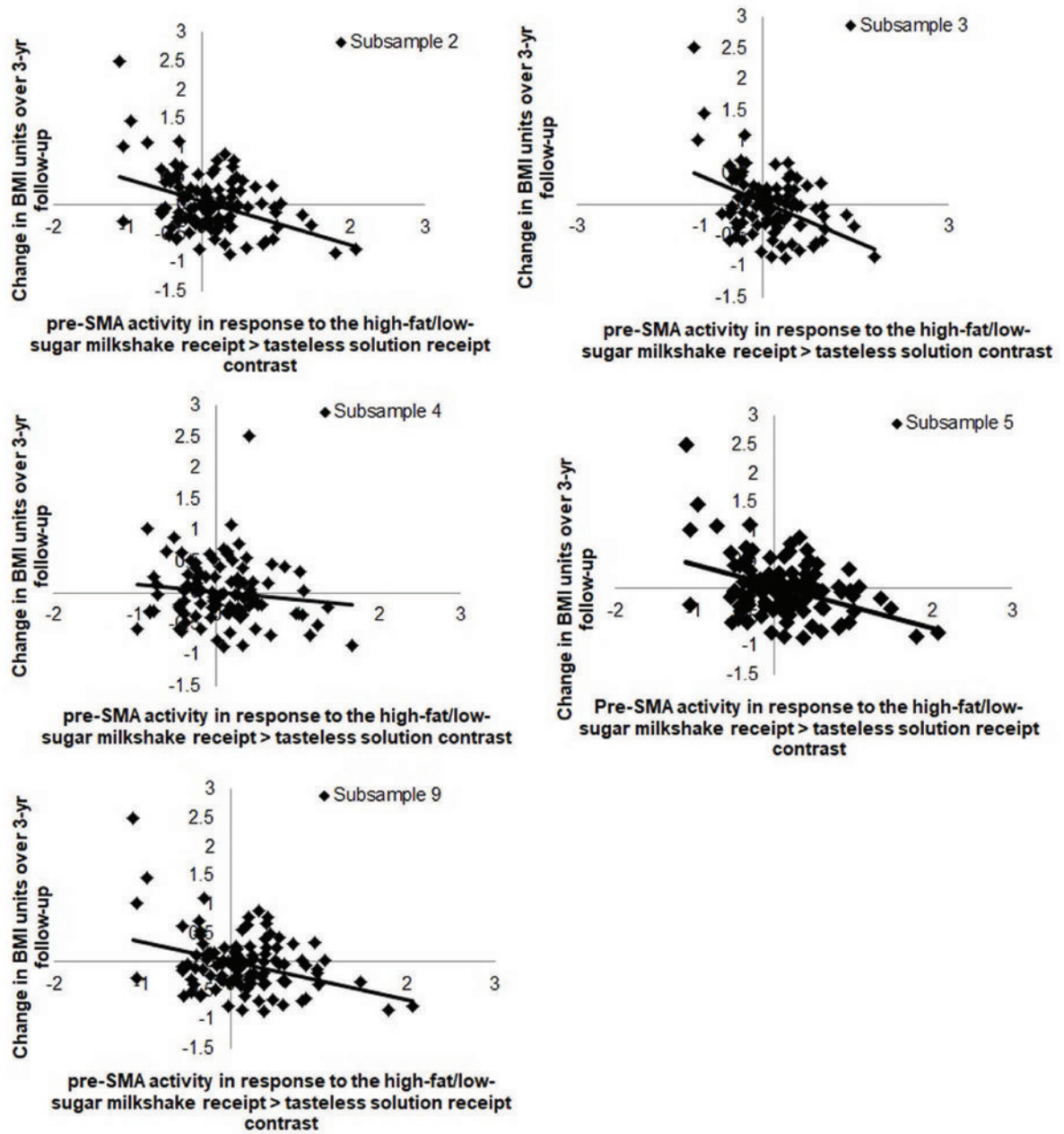
Figure 2.
BOLD activity in the pre-SMA to the high-fat/low-sugar milkshake receipt > tasteless
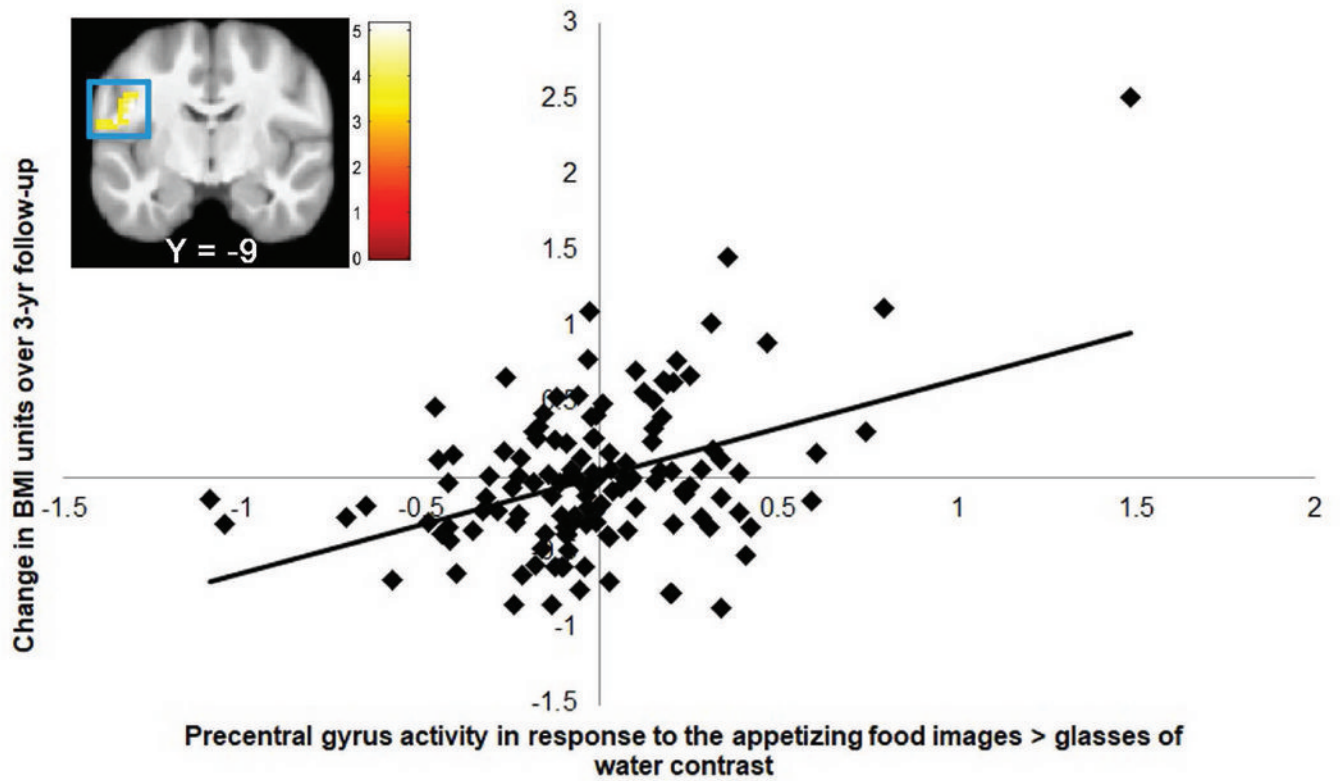solution contrast in 5 of the 10 subsamples.

Figure 3.
BOLD activity in the left precentral gyrus (MNI: –42, –9, 27, Z = 4.79, k = 72), extending into left Rolandic operculum to the appetizing food pictures > glasses of water contrast is positively associated with BMI gain over 3-year follow-up. The effects remained significant when excluding the outlier.
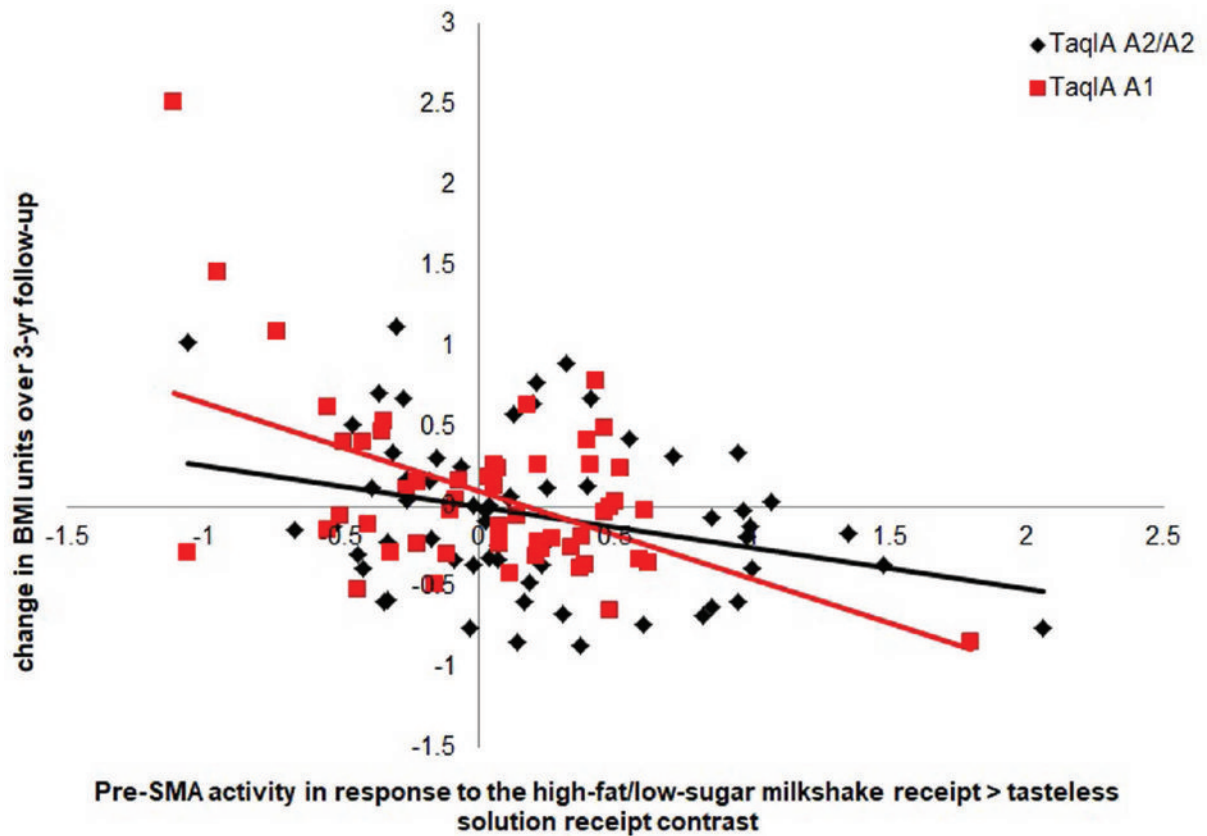
Figure 4.
TaqIA significantly moderated the effects of neural activation in the left pre-SMA (MNI coordinates: −3, 18, 54) in response to high-fat/low-sugar milkshake receipt > tasteless solution receipt on BMI gain. The interactive effects suggest that blunted pre-SMA activation in response to high-fat/low-sugar milkshake vs tasteless solution predicted greater BMI gain in A1 (r = −0.53, p<0.001) than A2/A2 carriers (r = −0.36, p<0.01).

Table 1.

Main effects for contrasts from the food image paradigm

Contrasts	k	Z value	MNI coordinates	Effect size r (Z/ N)
Appetizing food > unappetizing food				
Superior parietal lobe	1077	5.90	−9, −66, 57	0.51
Cuneus		5.71	−27, −81, 30	0.50
Precuneus		5.66	−12, −81, 45	0.49
Posterior cerebellar lobe	355	5.82	24, −66, −27	0.51
Posterior cerebellar lobe		4.35	−15, −69, −24	0.38
Posterior cerebellar lobe		4.30	3, −69, −24	0.37
Anterior cingulate cortex	146	5.42	−3, 9, 30	0.47
Supplemental motor area		4.90	0, 3, 48	0.43
Supplemental motor area		4.29	−3, −3, 57	0.37
Middle frontal gyrus	87	5.02	−27, −9, 57	0.44
Middle frontal gyrus		3.54	−24, 6, 60	0.31
Posterior cingulate cortex	187	4.95	−15, −57, 12	0.43
Anterior cerebellar lobe		4.65	6, −48, −6	0.40
Anterior cerebellar lobe		4.31	−3, −48, −3	0.37
Striatum	38	4.79	6, 21, 0	0.42
Cuneus	113	4.56	9, −93, 15	0.40
Cuneus		4.13	9, −90, 24	0.36
Cuneus		3.98	−6, −99, 6	0.35
Rolandic operculum	63	3.91	57, −12, 27	0.34
Rolandic operculum		3.69	54, −6, 18	0.32
Appetizing food > glasses of water				
Lingual gyrus	6993	Inf[*]	−3, −87, −12	>0.9
Lingual gyrus		Inf[*]	15, −90, −12	>0.9
Lingual gyrus		Inf[*]	9, −84, −12	>0.0
Mid insula	37	Inf[*]	−36, −6, 9	>0.9
Inferior frontal gyrus	165	Inf[*]	−51, 9, 27	>0.9
Inferior frontal gyrus		6.01	−51, 6, 39	0.52
Medial orbitofrontal cortex	35	7.52	−30, 36, −18	0.65
Inferior frontal gyrus	62	6.30	57, 9, 30	0.55
Inferior frontal gyrus		4.52	51, 6, 42	0.39
Supplemental motor area	144	5.40	0, 6, 57	0.47
Mid cingulate cortex		4.60	0, 15, 39	0.4-
Ventrolateral prefrontal cortex	50	4.80	−45, 39, 9	0.42
Inferior frontal gyrus		4.11	−51, 33, 15	0.36
Middle frontal gyrus		3.70	−51, 27, 24	0.32

*
 Z-value > 12.00. For all contrasts, activated regions, z-values and coordinates within the MNI coordinate system are displayed. Number of continuous voxels (*k*) are shown for peak coordinates. Peaks within the regions were considered significant at *k* > 34, P<0.05, corrected for multiple comparisons across the entire brain.

Table 2.

Pleasantness ratings of the 4 types of milkshake (N = 135)

Pleasantness ratings	Mean (SD)
High-fat/high-sugar milkshake	14.73 (3.19) [a]
High-fat/low-sugar milkshake	11.99 (3.84) [c]
Low-fat/high-sugar milkshake	12.94 (4.44) [b]
Low-fat/low-sugar milkshake	9.89 (3.96) [d]
Tasteless solution	10.59 (3.43) [d]

Different superscript letters indicate significant differences in pleasantness ratings ($P < 0.01$) assessed via within-subject t-tests.

Table 3.

Descriptive statistics for BMI values by Year

Year	M	SD	Range
Baseline BMI	21.2	2.3	16.2–26.4
1 Year Follow-Up	21.5	2.5	16.8–28.3
2 Year Follow-Up	22.1	2.8	17.0–31.3
3 Year Follow-Up	22.6	3.2	16.2–33.7

Table 4.

Correlations between BOLD Activation to Milkshake Receipt and Appetizing Food Pictures and BMI Gain over 3-year follow-up

Contrast and region	k	Z value	MNI coordinates	r (Z/ N)
High-fat/low-sugar milkshake receipt > tasteless solution receipt				
Negative correlation BMI gain				
Pre-Supplementary Motor Area	51	4.87	−3, 18, 54	−0.42
Appetizing food pictures > glasses of water				
Positive correlation BMI gain				
Precentral gyrus	72	4.79	−42, −9, 27	0.41
Rolandic operculum		3.62	−60, −9, 15	0.31
Appetizing food pictures > unappetizing food pictures				
Negative correlation BMI gain				
Ventromedial prefrontal cortex	43	4.08	12, 48, −3	−0.35
Medial orbitofrontal cortex		3.84	6, 45, −9	−0.33

For all contrasts, activated regions, z-values and coordinates within the MNI coordinate system are displayed. Number of continuous voxels (*k*) are shown for peak coordinates. Peaks within the regions were considered significant at p<0.001 uncorrected, *k* 37, P<0.05, corrected for multiple comparisons across the entire brain.

Table 5.

Correlations between BOLD Activation to Milkshake Receipt and Appetizing Food Pictures and BMI Gain over 3-year follow-up within the 10 subsamples

Contrast and region	*K*	Z value	MNI coordinates
High-fat/low-sugar milkshake receipt > tasteless solution receipt			
Negative correlation BMI gain			
Pre-Supplementary Motor Area	50	4.89	−3, 18, 54
Subsample 1	23	4.09	−3, 18, 54
Subsample 2	51	4.88*	−3, 18, 54
Subsample 3	39	4.85*	−3, 18, 54
Subsample 4	37	4.47*	−3, 18, 54
Subsample 5	54	4.81*	−3, 18, 54
Subsample 6	–	1.22	−6, 21, 51
Subsample 7	–	1.36	0, 24, 48
Subsample 8	–	1.73	0, 21, 45
Subsample 9	40	4.52*	−9, 21, 51
Subsample 10	–	1.36	0, 24, 48
Appetizing food pictures > glasses of water			
Positive correlation BMI gain			
Precentral gyrus	72	4.79	−42, −9, 27
Subsample 1	81	4.79*	−45, −9, 27
Subsample 2	47	4.70*	−45, −9, 27
Subsample 3	57	4.52*	−45, −9, 27
Subsample 4	13	4.54	−45, −6, 27
Subsample 5	91	4.84*	−45, −9, 27
Subsample 6	–	1.83	−51, −9, 21
Subsample 7	–	1.20	−42, −9, 36
Subsample 8	–	1.06	−45, −3, 30
Subsample 9	–	1.98	−42, −6, 36
Subsample 10	–	1.22	−45, −12, 42
Appetizing food pictures > unappetizing food pictures			
Negative correlation BMI gain			
Ventromedial prefrontal cortex	43	4.08	12, 48, −3
Subsample 1	12	3.62	12, 48, −3
Subsample 2	11	4.04	9, 48, −3
Subsample 3	58	4.33*	12, 48, −3
Subsample 4	–	3.33	12, 48, −3
Subsample 5	10	3.54	12, 48, −3
Subsample 6	–	–	–

Contrast and region	*K*	Z value	MNI coordinates
Subsample 7	–	0.82	12, 45, 6
Subsample 8	–	–	–
Subsample 9	–	2.13	9, 57, –6
Subsample 10	–	1.00	15, 51, –6

For all contrasts, activated regions, z-values and coordinates within the MNI coordinate system are displayed. Number of continuous voxels (k) are shown for peak coordinates. Peaks within the regions were considered significant at p<0.001 uncorrected, k   37, P<0.05, corrected for multiple comparisons across the entire brain.

*
 Activated regions significant at p<0.001 uncorrected, k   37 within the bootstrap samples.